Coupled Systems Mechanics, *Vol. 13, No. 6 (2024) 509-527*
https://doi.org/10.12989/csm.2024.13.6.509

Isogeometric finite element method for the dynamic analysis of functionally graded plates

Abdelhafid Lahdiri[1], Lazreg Hadji[2], Hassen Ait Atmane*[3] and Mohammed Kadri[4]

[1]Department of Technology, Faculty of Technology, University of Bejaia, 06000 Bejaia, Algeria
[2]Department of Civil Engineering, University of Tiaret, Algeria
[3]Laboratory of Structures, Geotechnics and Risks, Department of Civil Engineering, Faculty of Civil Engineering and Architecture, University Hassiba Benbouali of Chlef, Algeria
[4]Department of Civil Engineering, University of M'Hamed Bougara, Boumerdes, Algeria

(Received September 15, 2024, Revised December 16, 2024, Accepted December 17, 2024)

Abstract. This study investigated the free vibration behavior of functionally graded plates using iso-geometric finite element analysis (IGA). The effective material properties were estimated through the rule of mixtures, accounting for composition changes governed by a power law. To achieve this, an efficient computational framework based on IGA was developed, utilizing NURBS (Non-uniform Rational B-Spline) basis functions for structural discretization. The analysis focused on assessing the impact of geometry and material gradation parameters on the natural frequencies of square plates under various boundary conditions. Several numerical examples were presented to demonstrate the effectiveness of the proposed approach, and the results were validated by comparing them with other published models. The study covered both isotropic and functionally graded materials, specifically Al/Al2O3 and Al/ZrO2, to examine the variations in their natural frequency responses. The findings revealed a significant influence of boundary conditions on the frequency response of Al/Al2O3. The research thus provided important insights into the vibrational characteristics of different materials, considering various gradation schemes, geometrical modifications, and boundary conditions, offering valuable guidance for material selection in specific applications.

Keywords: free vibration; functionally graded materials; iso-geometric analysis; power law index

1. Introduction

Iso-geometric methods have been applied to analyze the static and dynamic behavior of rods, plane strain, and plane stress problems within the framework of simplified strain gradient elasticity theory, validating the method's applicability and accuracy (Balobanov *et al.* 2016). An advanced ANURBS-based isogeometric fluid-structure interaction formulation was also developed, allowing the coupling of incompressible fluids with non-linear elastic solids undergoing large displacements. This formulation was applied to arterial blood flow simulations and validated using benchmark problems as well as patient-specific computations of the abdominal aorta (Bazilevs *et al.* 2006).

*Corresponding author, Professor, E-mail: h.aitatmane@univ-chlef.dz

http://www.techno-press.org/?journal=csm&subpage=8 ISSN: 2234-2184 (Print), 2234-2192 (Online)

Another significant contribution introduced a novel numerical method based on the scaled boundary finite-element method (SB-FEM) to address in-plane motion problems in elastic solids. This approach discretizes only the boundary of the element, with the interior domain being described by a radial scaling factor. The governing equations are transformed into a scaled boundary finite element formulation, and the iso-geometric collocation method is applied to solve them (Chen *et al*. 2014).

In the field of structural vibrations, iso-geometric analysis was applied to various models, including rods, beams, membranes, plates, and solids. It was found that the *k*-method offered more accurate frequency spectra than higher-order finite elements. Nonlinear parameterizations showed promise in eliminating optical branches and mitigating accuracy loss. A geometric model of NASA's Aluminum Testbed Cylinder was created, demonstrating satisfactory alignment with experimental data, though mass lumping remains a challenge for preserving higher-order accuracy (Cottrell *et al.* 2006, Hughes *et al.* 2005).

Iso-geometric analysis has demonstrated significant effectiveness in solving linear structural and fluid mechanics problems, achieving strong convergence and precision. Key future research areas include further integration with CAD, mesh generation, unstructured elements, shell analysis, dynamic analysis, contact problems, fluid mechanics, and broader engineering applications (Hughes *et al.* 2010). Moreover, IGA was implemented in Matlab, where the authors discussed element concepts, data processing, and object-oriented programming for greater versatility. Several examples highlighted IGA's convergence properties and its advantages over traditional Finite Element Method (FEM) approaches (Kacprzyk and Ostapska-Łuczkowska 2014).

Free vibration analysis using Iso-geometric approach (IGA), a spline-based FEM was performed and its results was compared with FEM, Rayleigh-Ritz method, and experimental data for benchmark tests on block and cylinder models. Convergence rate, accuracy, and computational time are compared between IGA and FEM, considering spline order and parameterization effects. The paper also discusses the potential of IGA in Resonant Ultrasound Spectroscopy for measuring elastic properties of anisotropic solids (Kolman *et al.* 2015). Introduces iso-geometric analysis as a comparable tool to the finite element method, offering the advantage of accurately representing mesh geometry through a connection between CAD and NURBS shape functions (Rauen *et al.* 2013). Numerical experiments are conducted on 1-D, 2-D and 3D structural problems to assess IGA's performance in analyzing natural frequencies and modes (Hughes *et al.* 2010). This study presents an isogeometric finite element method for analyzing natural frequencies in thin plate problems with various geometries. Non-Uniform Rational B-Splines (NURBS) basis functions are used to approximate the deflection field of the thin plate and describe its geometry. The governing equations for the free vibration of Kirchhoff thin plates are derived using the Galerkin method (Shojaee *et al*. 2012). Alghanmi (2022) studied the static analysis of functionally graded (FG) nanoplates with porosities, using a model that combines the nonlocal strain gradient theory with the four-variable shear deformation theory. The buckling and porosity effect of multilayered and structural behaviour of magneto-electro-elastic plate have find in the works of (Kiran and Kattimani 2017, 2018a, 2018b). The free vibration, static and porosity effect of functionally graded skew magneto-electro-elastic plate are developed in the papers of (Kiran and Kattimani 2018c, 2018d, 2018e, 2018f). Bennai *et al.* (2019) studied free vibration response of functionally graded Porous plates using a higher-order Shear and normal deformation theory. Hussain and Selmi (2020) investigated effect of Pasternak foundation: Structural modal identification for vibration of FG shell. Khadimallah *et al.* (2021) studied the effects of nonlocal parameter on bending of Intermediate filaments: Formulation of Euler beam theory. Alghanmi (2024) examines the static bending behavior of sandwich plates made of functionally graded materials, specifically focusing on different representations of porosity distribution throughout their thickness.

Later, authors performed static analysis on a thin plate by employing isogeometric method, the essential boundary condition was employed using Lagrange multiplier method (Shojaee and Valizadeh 2012). To overcome numerical locking, the researchers introduce an effective isogeometric approach that combines in-plane and out-of-plane patterns, enabling precise analysis of the vibration behavior in curved beams (Liu *et al.* 2016). Performed an isogeometric analysis and X-FEM to accurately model crack problems, using NURBS functions for geometry and enrichment functions for crack identification and solution improvement (Shojaee *et al.* 2013). Analyzed free vibration behavior of functionally graded plates with straight and curved embedded cracks using a NURBS-based multi-patch isogeometric analysis. Material and geometry parameters are examined, and the influence of crack characteristics on vibration modes is investigated (Khalafi and Fazilati 2021). Selmi (2021) developed free vibration of bi-dimensional functionally graded simply supported beams. Bennai *et al.* (2022) developed the wave dispersion and vibration characteristics of FG plates resting on elastic Kerr foundations via HSDT. Alghanmi (2023) explored, for the first time, the bending behavior of sandwich nanoplates consisting of a functionally graded (FG) porous core and electromagnetic layers, utilizing a nonlocal strain gradient theory combined with a four-unknown shear deformation theory. Kiani and Arefi (2023) used Nonlocal bending characteristics of nanoplate reinforced by functionally graded GPLs exposed to thermo-mechanical loads resting on the Pasternak's foundation. Lakel *et al.* (2024) developed the natural frequency of FG-GNPR nanoplates under different boundary conditions. Draouche *et al.* (2024) studied effect of porosity and boundary conditions on dynamic characteristics of cracked plates made of functionally graded materials. Meski *et al.* (2024) used a new quasi-3D HSDT for static behavior of functionally graded sandwich beam with 1D-FG skins and ceramic core. Ould Larbi *et al.* (2024) investigated a simple refined plate theory for buckling problems of in-plane bi-directional functionally graded plates with porosity under various boundary conditions. Zouatnia *et al.* (2024) examines impact of porosity distribution and grading parameters on free vibration of functionally graded beams. Djebbour *et al.* (2024) investigated the effect of porosity distribution on free vibration of functionally graded plates: an accurate application of HSDT theory. Actually, Lahdidi and Kadri (2022) analyse the free vibration behaviour of multi-directional functionally graded imperfect plates using 3D isogeometric approach. This paper proposes a density-based topology optimization method using isogeometric analysis for generating supports in additive manufacturing. Two cases are examined: separate support design and support design within optimized main structures. The method considers gravity loads and demonstrates efficient support generation (Kazemi and Tavakkoli 2023).

A comprehensive investigation was undertaken to analyze the behavior of functionally graded plates during free vibration using iso-geometric finite element analysis. The study utilized the rule of mixture to estimate effective material properties based on power law composition changes. To achieve this, a highly efficient computational method was developed using IGA and NURBS (Non-uniform rational B-spline) basis functions for structural discretization. The functionally graded plate structure analysed in the study has diverse applications in industries such as aerospace, mechanical, civil, biomedical, and energy systems. By tailoring material properties along the plate, it optimizes performance under varying conditions like thermal gradients, mechanical stresses, and loading. This makes it ideal for components such as turbine blades, aerospace structures, prosthetics, and energy devices, where enhanced durability, efficiency, and performance are required. The main focus of the study was to examine how the natural frequency

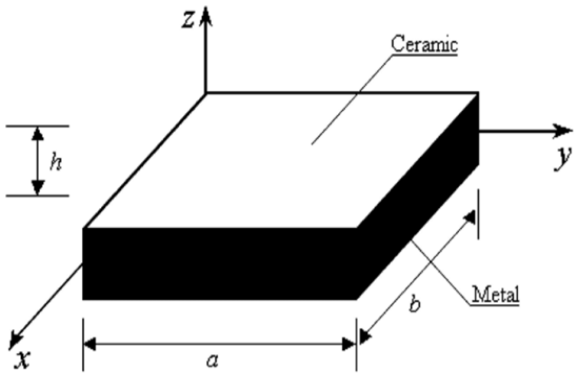

Fig. 1 Geometry of rectangular plate composed of FGM

of a square plate is affected by different geometry and grading parameters, considering various boundary conditions. A wide range of numerical examples were provided to demonstrate the effectiveness of the proposed formulation, and comparisons were made with other existing models to validate the accuracy of the results. Both isotropic and functionally graded materials, specifically Al/Al_2O_3 and Al/ZrO_2, were extensively studied to understand their distinct natural frequency responses. The research findings emphasized that the choice of boundary conditions had a significant impact on the frequency behavior of Al/Al_2O_3 plates. Consequently, the study provided valuable insights into the frequency response of different materials, considering various gradations, changes in geometry, and boundary conditions. These insights can be instrumental in selecting the most suitable materials for specific applications. Isogeometric finite element analysis (IGA) offers several key benefits for structural analysis, particularly in studying complex materials and geometries like functionally graded plates. By using Non-uniform rational B-splines (NURBS) for discretization, IGA enables a seamless transition between design and analysis, providing high accuracy with fewer degrees of freedom. This results in improved computational efficiency, especially when investigating natural frequency behaviors, as seen in the study of functionally graded materials. IGA's ability to handle intricate material gradations and geometric complexities, while offering precise results with minimal computational cost, makes it an effective tool for analyzing dynamic responses, including vibration frequencies under various boundary conditions.

2. Problem formulation

2.1 Geometrical configuration

Consider a plate of total thickness ***h*** and composed of functionally graded material through the thickness (Fig. 1). It is assumed that the material is isotropic and grading is assumed to be only through the thickness. The *xy* plane is taken to be the undeformed mid plane of the plate with the *z* axis positive upward from the mid plane.

2.2 Material properties

The functionally graded materials are materials in which the material composition varying

Table 1 Material properties (Benachour *et al.* 2011)

Material	Properties		
	E (GPa)	ν	ρ (Kg/m^3)
Aluminum (Al)	70	0.3	2702
Alumina (Al_2O_3)	380	0.3	3800
Zirconia (ZrO_2)	200	0.3	5700

gradually from one material to another generally from metal to ceramic. In order to take advantage of both materials without having a boundary between the two that creates a fragility area, the FGMs vary generally along a single axis (the Z-axis) and the properties of the materials are given as a function of the variation volume of ceramic by (Ait Atmane *et al.* 2010)

$$E(z) = (E_c - E_m)V_c + E_m \tag{1}$$

$$\rho(z) = (\rho_c - \rho_m)V_c + \rho_m \tag{2}$$

Where, E and ρ represent the Young's modulus and the density of the constituents of structure.The fraction of volume ceramic is given as a function of height and spatial position z. The axis of coordinates z is located on the median plane of the plate where $-\frac{h}{2} \leq z \leq \frac{h}{2}$.

Now, the total volume fraction of the metal and ceramic is: $V_m + V_c = 1$, and the power law of volume fraction of the ceramic is described as (Ait Atmane *et al.* 2010)

$$V_c = \left(\frac{z}{h} + \frac{1}{2}\right)^p \tag{3}$$

Where p the power law index of the fraction of volume variation is, $p = 0$ is a fully ceramic plate, $p = \infty$ is a fully metal plate.

The material properties of the metal and ceramic given by Benachour *et al.* (2011) are summarized in the Table 1.

3. Isogeometric analysis

3.1 NURBS functions

Isogeometric analysis is a finite element modelling method, first introduced by Hughes *et al.* in 2005 (Hughes *et al.* 2005), with the idea of removing the gap between the computer-aided design and the analysis model (Cottrell *et al.* 2009). In the classical finite element, modelling the CAD models is translated for analysis, which constitutes important calculation time. In the isogeometric method, the CAD model is directly used for the analysis, for this the standard polynomial shape functions of the classical FEM are replaced by the CAD shape function (Cottrell *et al.* 2006), the CAD shape functions are parametric piecewise functions. Several CAD formulations can be used in isogeometric methods, but the most used in engineering are the NURBS (Non-uniform rational B-spline) (Cottrell *et al.* 2009), which are a generalization of the B-spline.

For the construction of the *b*-spline we need the node vector, which is a vector containing the coordinates in the parameter space, it is an increasing vector which is defined by $\Xi = \{\xi_1, \xi_2, \dots, \xi_{n+p+1}$ where n is the number of shape functions, p is the order of the functions and ξ_i

is the i^{th} node where $\xi_i \in \mathbb{R}$ (Cottrell *et al.* 2009).

The b-spline is constructed by recurrence according to the functions of lower order; it is given by the formula of cox (COX 1971) and de boor (De Boor 1972) and write as

For $p = 0$

$$N_{i,p} = \begin{cases} 1 & if \quad \xi_i \leq \xi \leq \xi_{i+1} \\ 0 & otherwise \end{cases} \tag{4}$$

For $p \geq 1$

$$N_{i,p} = \frac{\xi - \xi_i}{\xi_{i+p} - \xi_i} N_{i,p-1}(\xi) + \frac{\xi_{i+p+1} - \xi}{\xi_{i+p+1} - \xi_{i+1}} N_{i+1,p-1}(\xi) \tag{5}$$

NURBS are generalizations of b-spline, they are efficient for modelling, especially for conical and cylindrical sections, which are exactly reproduced, they are given in terms of b-spline functions rationalized by weights w_i , (Les and Wayne 1997) the NURBS equations are written as

$$R_{i,j,k}^{p,q,r}(\xi,\eta,\zeta) = \frac{N_{i,p}(\xi) M_{j,q} L_{k,r}(\zeta) w_{i,j,k}}{\sum_{\hat{i}=1}^{n} \sum_{\hat{j}=1}^{m} \sum_{\hat{k}=1}^{l} N_{\hat{i},p}(\xi) M_{\hat{j},q}(\eta) L_{\hat{k},r}(\zeta) w_{\hat{i},\hat{j},\hat{k}}} \tag{6}$$

The NURBS solid cross-sections are given by the trilinear combination of the NURBS shape functions and the control points. It is expressed as (Cottrell, Hughes *et al.* 2009)

$$S(\xi,\eta,\zeta) = R_{i,j,k}^{p,q,r}(\xi,\eta,\zeta) B_{i,j,k} \tag{7}$$

The derivatives of the b-spline functions are given by the lower-order functions and are written as (Cottrell *et al.* 2009)

$$\frac{d}{d\xi} N_{i,p}(\xi) = \frac{p}{\xi_{i+p} - \xi} N_{i,p-1}(\xi) - \frac{p}{\xi_{i+p+1} - \xi_{i+1}} N_{i+1,p-1}(\xi) \tag{8}$$

3.2 Three-dimensional elasticity formulation

The stress-strain relationship is given by the Cauchy tensor

$$\sigma_{i,j} = 2\mu\varepsilon_{ij} - \lambda\delta_{i,j} \tag{9}$$

The μ and λ are the lamé's coefficients given as a function of the Young modulus and Poisson coefficient and are written as (Cazenave 2010)

$$\lambda = \frac{\nu E}{(1+\nu)(1-2\nu)} \tag{10}$$

$$\mu = \frac{E}{2(1+\nu)} \tag{11}$$

Where E and ν are the Young's modulus and Poisson coefficient respectively.

The strains for the case of linear elasticity in small deformation are given as a function of the displacements by

$$\varepsilon_{i,j} = \frac{1}{2}\left(u_{i,j} + u_{j,i}\right) \tag{12}$$

Where $u_{i,j}$ and $u_{j,i}$ are the derivative of the displacement field in direction j and i.

The approximation of the displacement field is given by using the NURBS functions as interpolation function; the displacement field is then given by (Buffa and Sangalli 2016)

$$u \approx RU \tag{13}$$

Where R is the NURBS shape function matrix, u is the displacement field with $u = \{u_1, u_2, u_3\}$ and U is the vector of control points.

The stress-strain relationship then becomes in its matrix form

$$\begin{Bmatrix} \sigma_{11} \\ \sigma_{22} \\ \sigma_{33} \\ \sigma_{12} \\ \sigma_{23} \\ \sigma_{13} \end{Bmatrix} = \begin{bmatrix} d_1 & d_1 & d_2 & 0 & 0 & 0 \\ d_2 & d_1 & d_2 & 0 & 0 & 0 \\ d_2 & d_2 & d_1 & d & 0 & 0 \\ 0 & 0 & 0 & d_3 & 0 & 0 \\ 0 & 0 & 0 & 0 & d_3 & 0 \\ 0 & 0 & 0 & 0 & 0 & d_3 \end{bmatrix} \begin{Bmatrix} \varepsilon_{11} \\ \varepsilon_{22} \\ \varepsilon_{33} \\ 2\varepsilon_{12} \\ 2\varepsilon_{23} \\ 2\varepsilon_{13} \end{Bmatrix} \tag{14}$$

Where the factors d_1 , d_2 and $d_3$are given in terms of Young's modulus and Poisson's ratio by

$$d_1 = \frac{E(1-\nu)}{(1+\nu)(1-2\nu)} \tag{15}$$

$$d_2 = \frac{E\nu}{(1+\nu)(1-2\nu)} \tag{16}$$

$$d_3 = \frac{E}{2(1+\nu)} \tag{17}$$

The stiffness matrix is then given by the integral

$$K = \int_\Omega B^T D B d\Omega \tag{18}$$

Where D is the elastic matrix given in the Eq. (14). The mass matrix is then given by the integral

$$M = \int_\Omega R^T \rho R d\Omega \tag{19}$$

The eigenvalue and eigenvector problem is then given by

$$([K] - \omega^2[M])\{\Delta\} = \{0\} \tag{20}$$

The boundary conditions are given for a simple support plate by (Son and Huu-Tai 2019)

$$\begin{aligned} u_1 = u_2 = u_3 = 0 \quad &\text{at} \quad y = 0, b \\ u_1 = u_2 = u_3 = 0 \quad &\text{at} \quad x = 0, a \end{aligned} \tag{21}$$

and for clamped support the boundary is given by

$$u_1 = u_2 = u_3 = 0 \tag{22}$$

4. Result and discussion

Table 2 demonstrates the frequency of Al/Al_2O_3 graded plates for the SSSS boundary condition. The table illustrates that as the ratio of the plate thickness to the plate length (*h/a*) increases, the frequency of the plate decreases. Essentially, the higher *h/a* values indicate a thicker

Table 2 Comparison study of frequency parameter for SSSS Al/Al_2O_3 square plates ($b/a = 1$)

			FIRST MODE			SECOND MODE		
			h/a			h/a		
	Material	Method	0.05	0.1	0.2	0.05	0.1	0.2
Fully ceramic	10^{-3}	IGA	5.9236	5.7770	5.3063	14.6696	13.8221	11.6681
		REF1	5.9191	5.7728	5.2954	14.6110	13.789	11.6120
	10^{-4}	IGA	5.9256	5.7788	5.3079	14.6744	13.8264	11.6714
		REF1	5.9212	5.7748	5.2972	14.6160	13.794	11.6150
	10^{-5}	IGA	5.9258	5.7790	5.3081	14.6749	13.8269	11.6717
		REF1	5.9214	5.7751	5.2974	14.6160	13.795	11.6160
	10^{-6}	IGA	5.9258	5.7790	5.3081	14.6749	13.8269	11.6718
		REF1	5.9214	5.7751	5.2974	14.616	13.795	11.616
Fully metallic	10^{2}	IGA	3.0224	2.9474	2.7066	7.4846	7.0511	5.9501
		REF1	3.1833	3.1002	2.8315	7.8518	7.3875	6.1756
	10^{3}	IGA	3.0161	2.9415	2.7017	7.4694	7.0377	5.9408
		REF1	3.0329	2.9575	2.7115	7.4858	7.0622	5.9416
	10^{4}	IGA	3.0161	2.9415	2.7017	7.4694	7.0377	5.9408
		REF1	3.0139	2.9413	2.6978	7.4443	7.0254	5.9152
	10^{5}	IGA	3.0161	2.9415	2.7017	7.4694	7.0377	5.9408
		REF1	3.0139	2.9394	2.6963	7.4396	7.0212	5.9123

REF1: (Hosseini-Hashemi *et al.* 2011)

Table 3 Comparison study of frequency parameter for SCSF Al/Al_2O_3 square plates ($b/a = 1$)

			FIRST MODE			SECOND MODE		
			h/a			h/a		
	Material	Method	0.05	0.1	0.2	0.05	0.1	0.2
Fully ceramic	10^{-3}	IGA	3.8097	3.7173	3.4537	9.8329	9.2703	7.881
		REF1	3.7958	3.7088	3.4464	9.7515	9.2185	7.8347
	10^{-4}	IGA	3.8110	3.7186	3.4548	9.8361	9.2732	7.8832
		REF1	3.7971	3.7101	3.4476	9.755	9.2216	7.8372
	10^{-5}	IGA	3.8111	3.7187	3.4549	9.8364	9.2735	7.8835
		REF1	3.7973	3.7102	3.4476	9.7553	9.222	7.8375
	10^{-6}	IGA	3.8111	3.7187	3.4549	9.8364	9.2735	7.8835
		REF1	3.7973	3.7102	3.4477	9.7554	9.2220	7.8369
Fully metallic	10^{2}	IGA	1.9438	1.8966	1.7618	5.0168	4.7291	4.0191
		REF1	2.0414	1.9918	1.8447	5.2399	4.939	4.1713
	10^{3}	IGA	1.9398	1.8928	1.7585	5.0066	4.7201	4.0126
		REF1	1.9449	1.9001	1.7648	4.9963	4.7214	4.0089
	10^{4}	IGA	1.9398	1.8928	1.7585	5.0066	4.7201	4.0126
		REF1	1.9449	1.8896	1.7558	4.9687	4.6967	3.9909
	10^{5}	IGA	1.9398	1.8928	1.7585	5.0066	4.7201	4.0126
		REF1	1.9328	1.8885	1.7548	4.9654	4.6939	3.9889

REF1: (Hosseini-Hashemi *et al.* 2011)

Table 4 Comparison of the natural frequency parameter for SSSS Al/Al_2O_3 square plates ($b/a = 1$)

			Power law index (P)					
h/a	(m,n)	METHOD	0	0.5	1	4	10	∞
0.05	(1,1)	IGA	0.0148	0.0126	0.0113	0.0098	0.0094	-
		REF1	0.0148	0.0125	0.0113	0.0098	0.0094	-
		REF2	0.0146	0.0124	0.0112	0.0097	0.0093	-
		REF3	0.0148	0.0128	0.0115	0.0101	0.0096	
0.1	(1,1)	IGA	0.0578	0.0492	0.0443	0.0381	0.0363	0.0294
		REF1	0.0577	0.049	0.0442	0.0382	0.0366	0.0293
		REF4	0.0577	0.0492	0.0443	0.0381	0.0364	0.0293
		REF2	0.0568	0.0482	0.0435	0.0376	0.0359	-
		REF3	0.0577	0.0492	0.0445	0.0383	0.0363	0.0294
	(1,2)	IGA	0.1383	0.1182	0.1064	0.0906	0.0858	0.0704
		REF1	0.1376	0.1173	0.1059	0.0911	0.0867	0.0701
		REF4	0.1381	0.118	0.1063	0.0904	0.0859	0.0701
		REF2	0.1354	0.1154	0.1042	-	0.085	-
	(2,2)	IGA	0.2125	0.1822	0.1642	0.1385	0.1305	0.1082
		REF1	0.2112	0.1805	0.1631	0.1397	0.1324	0.1076
		REF4	0.2121	0.1819	0.164	0.1383	0.1306	0.1077
		REF2	0.2063	0.1764	0.1594	-	0.1289	-
0.2	(1,1)	IGA	0.2123	0.1821	0.1641	0.1383	0.1304	0.1081
		REF1	0.2112	0.1805	0.1631	0.1397	0.1324	0.1076
		REF4	0.2121	0.1819	0.164	0.1383	0.1306	0.1077
		REF2	0.2055	0.1757	0.1587	0.1356	0.1284	-
		REF3	0.2112	0.1806	0.165	0.1371	0.1304	0.1075
	(1,2)	IGA	0.4669	0.404	0.365	0.3005	0.2792	0.2376
		REF1	0.4618	0.3978	0.3604	0.3049	0.2856	0.2352
		REF4	0.4658	0.404	0.3644	0.3	0.279	0.2365
	(2,2)	IGA	0.6775	0.5897	0.5338	0.4337	0.399	0.3448
		REF1	0.6676	0.5779	0.5245	0.4405	0.4097	0.3399
		REF4	0.6753	0.5891	0.5444	0.4362	0.3981	0.3429

REF1: (Hosseini-Hashemi *et al.* 2011) REF2: (Zhao *et al.* 2009), REF3 (Hosseini-Hashemi *et al.* 2010), REF4: (Matsunaga 2008)

plate that is less flexible, resulting in a lower frequency of vibration. Moving on to Table 3, it represents the frequency data for SCSF plates. In comparison to the SSSS boundary condition, the SCSF plates exhibit lower frequencies. This means that SCSF plates vibrate at lower natural frequencies compared to SSSS plates. The decrease in frequency with increasing h/a ratio can be attributed to the increased stiffness and mass distribution, which reduces the plate's ability to vibrate at higher frequencies. Thicker plates resist deformation more, making them less responsive to vibrational forces. In contrast, SCSF plates, with their more flexible boundary conditions, allow greater displacement at the edges, which results in lower natural frequencies. This indicates that boundary conditions play a crucial role in the vibrational characteristics of functionally graded plates.

Table 5 Comparison of fundamental frequency parameter for SSSS Al/ZrO_2 square plates (*b/a*=1)

method	$p=0$		$p=1$			$h/a=0.2$		
	$h/a=1/\sqrt{10}$	$h/a=0.1$	$h/a=0.05$	$h/a=0.1$	$h/a=0.2$	$p=2$	$p=3$	$P=5$
IGA	0.4667	0.0578	0.0159	0.062	0.2287	0.2266	0.2272	0.2282
REF1	0.4618	0.0577	0.0158	0.0619	0.2276	0.2264	0.2276	0.2291
REF4	0.4658	0.0577	0.0158	0.0619	0.2285	0.2264	0.227	0.2281
REF5	0.4658	0.0577	0.0153	0.0596	0.2192	0.2197	0.2211	0.2225
REF6	0.4658	0.0578	0.0157	0.0613	0.2257	0.2237	0.2243	0.2253
REF6	0.4619	0.0577	0.0162	0.0633	0.2323	0.2325	0.2334	0.2334
REF3	0.4618	0.0576	0.0158	0.0611	0.227	0.2249	0.2254	0.2265

REF1: (Hosseini-Hashemi *et al.* 2011), REF4: (Matsunaga 2008), REF5: (Vel and Batra 2004), REF6: (Pradyumna and Bandyopadhyay 2008)

Table 6 Comparison of first four natural frequency parameter for SSSS Al/Al_2O_3 plates (*b/h*=2)

h/a	Mode	method	Power law index (P)						
			0	0.5	1	2	5	8	10
0.05	B1	IGA	3.7168	3.1574	2.8392	2.5805	2.4424	2.3917	2.3578
		REF1	3.7123	3.1456	2.8352	2.5777	2.4425	2.3948	2.3642
	B2	IGA	5.9546	5.0623	4.5536	4.1375	3.9093	3.8257	3.7711
		REF1	5.9198	5.0175	4.5228	4.1115	3.8939	3.817	3.7681
	B3	IGA	9.8321	8.3808	7.5485	6.854	6.4433	6.293	6.2004
		REF1	9.5668	8.1121	7.3132	6.6471	6.2903	6.1639	6.0843
	B4	IGA	12.5289	10.6604	9.5906	8.7077	8.2062	8.0246	7.9099
		REF1	12.456	10.566	9.5261	8.6572	8.1875	8.0207	7.9166
0.1	B1	IGA	3.6562	3.1102	2.7974	2.5395	2.3932	2.3405	2.3073
		REF1	3.6518	3.0983	2.7937	2.5386	2.3998	2.3504	2.3197
	B2	IGA	5.7869	4.9288	4.4344	4.0218	3.7769	3.6898	3.6372
		REF1	5.7693	4.8997	4.4192	4.0142	3.7881	3.7072	3.658
	B3	IGA	9.2832	7.9251	7.1354	6.462	6.032	5.8813	5.7642
		REF1	9.1876	7.8145	7.0512	6.4015	6.0247	5.8887	5.8086
	B4	IGA	11.8839	10.1513	9.1388	8.2685	7.6984	7.5013	7.3937
		REF1	11.831	10.074	9.0928	8.2515	7.7505	7.5688	7.4639
0.2	B1	IGA	3.4533	2.952	2.6579	2.4031	2.2322	2.1736	2.1424
		REF1	3.4409	2.9322	2.6473	2.4017	2.2528	2.1985	2.1677
	B2	IGA	5.3103	4.5541	4.1036	3.7013	3.4071	3.3084	3.2604
		REF1	5.2802	4.5122	4.0773	3.6953	3.4492	3.3587	3.3094
	B3	IGA	8.1547	7.025	6.3382	5.6998	5.1843	5.0149	4.9406
		REF1	8.071	6.9231	6.2636	5.6695	5.2579	5.1045	5.0253
	B4	IGA	9.7417	8.7413	7.9619	7.1471	6.2962	5.9028	5.7486
		REF1	9.7416	8.6926	7.8711	7.1189	6.5749	5.9062	5.7518

REF1: (Hosseini-Hashemi *et al.* 2011)

Table 7 Comparison of first four natural frequency parameter for SSSC Al/Al_2O_3 square plates (b/h=1)

h/a	Mode	method	Power law index (P)						
			0	0.5	1	2	5	8	10
0.05	B1	IGA	7.0954	6.0336	5.4271	4.9295	4.6527	4.5518	4.4869
		REF1	7.0526	5.981	5.3926	4.9019	4.6382	4.5443	4.4854
	B2	IGA	15.3407	13.0596	11.7502	10.6639	10.0335	9.8065	9.6662
		REF1	15.243	12.937	11.667	10.601	10.016	9.8068	9.6779
	B3	IGA	17.4056	14.8346	13.3534	12.1126	11.3649	11.0966	10.9363
		REF1	17.175	14.588	13.159	11.956	11.283	11.04	10.893
	B4	IGA	25.197	21.488	19.3426	17.5328	16.4157	16.0192	15.7883
		REF1	24.951	21.208	19.136	17.38	16.379	16.016	15.8
0.1	B1	IGA	6.8173	5.8174	5.2368	4.7436	4.4309	4.321	4.2588
		REF1	6.7751	5.7649	5.2039	4.7261	4.4462	4.3439	4.2839
	B2	IGA	14.3438	12.275	11.0563	9.9909	9.2554	9.0041	8.8739
		REF1	14.254	12.158	10.982	9.9616	9.3302	9.0985	8.9685
	B3	IGA	15.957	13.6896	12.3409	11.1365	10.2503	9.9498	9.8035
		REF1	15.781	13.491	12.199	11.063	10.325	10.048	9.898
	B4	IGA	22.6521	19.4726	17.5616	15.8211	14.4799	14.0326	13.674
		REF1	22.425	19.205	17.372	15.741	14.643	14.044	13.672
0.2	B1	IGA	6.026	5.1926	4.6867	4.2162	3.8347	3.7086	3.6531
		REF1	5.9625	5.1188	4.6356	4.1996	3.8916	3.7746	3.7146
	B2	IGA	11.5666	10.343	9.35	8.3788	7.4606	6.9981	6.8174
		REF1	11.786	10.165	9.2165	8.331	7.6567	7.4012	7.2768
	B3	IGA	12.7653	11.112	10.0635	9.0008	7.9821	7.6554	7.5334
		REF1	12.543	10.865	9.8739	8.9239	8.1442	7.8438	7.7031
	B4	IGA	17.5169	15.2894	13.8599	12.3797	10.906	10.4339	10.2643
		REF1	17.199	14.93	13.571	12.249	11.142	10.717	10.521

REF1: (Hosseini-Hashemi *et al.* 2011)

Finally, Table 4 displays the effect of increasing the exponent p, on the overall composition of a ceramic and metal. As the exponent p increases, the overall composition of the ceramic decreases, while that of the metal increases. This implies that the relative proportion of ceramic material decreases while the proportion of metal material increases. The power law index increases, the stiffness of the plate becomes more concentrated at the surfaces, leading to a higher natural frequency due to the increased stiffness and reduced flexibility of the plate. This change in composition leads to a transition in material properties, such as increased ductility and thermal conductivity from the metal, while reducing stiffness and thermal resistance from the ceramic. As a result, the overall mechanical performance, vibration response, and thermal behavior of the plate are influenced, with the plate potentially becoming more flexible and less thermally resistant as the metal content increases.

Table 5 demonstrate the variation of frequency with different h/a and p for Al/ZrO_2. The effect of h/a on the frequency is significant compared to the grading parameter p. It is worth noting that for lower values of p the decrement in frequency is more and for higher values of p the difference in the results is very less. This indicates that the grading parameter p plays a more pronounced role

Table 8 Comparison of first four natural frequency parameter for SCSC Al/Al_2O_3 square plates (b/h=1)

h/a	Mode	method	Power law index (P)						
			0	0.5	1	2	5	8	10
0.05	B1	IGA	8.6817	7.3905	6.6503	6.0372	5.6822	5.5535	5.4737
		REF1	8.5674	7.2715	6.5585	5.9612	5.6332	5.5152	5.4423
	B2	IGA	16.2152	13.8123	12.43	11.2773	10.5943	10.349	10.2003
		REF1	16.065	13.642	15.39	11.181	10.555	10.33	10.193
	B3	IGA	20.5222	17.5232	15.7851	14.3065	13.3638	13.0271	12.836
		REF1	20.05	17.051	12.305	13.981	13.167	12.869	12.693
	B4	IGA	27.5566	23.5343	21.1966	19.2008	17.9153	17.4605	17.2058
		REF1	27.1	23.06	20.816	18.904	17.785	17.376	17.136
0.1	B1	IGA	8.169	6.9904	6.2984	5.6959	5.2806	5.1366	5.0614
		REF1	8.0702	6.8847	6.2222	5.6494	5.293	5.1594	5.0844
	B2	IGA	14.9918	12.8475	11.5776	10.4539	9.6501	9.377	9.2401
		REF1	14.862	12.693	11.472	10.405	9.7255	9.4734	9.3348
	B3	IGA	14.9918	12.8475	11.5776	10.4539	9.6501	9.377	9.2401
		REF1	17.918	15.371	13.921	12.621	11.714	11.366	11.186
	B4	IGA	24.2012	20.8601	18.8319	16.9429	15.4071	14.8981	14.6737
		REF1	23.85	20.475	18.543	16.799	15.566	15.098	14.858
0.2	B1	IGA	6.8821	5.9645	5.3948	4.8388	4.3397	4.1772	4.1122
		REF1	6.7663	5.8409	5.3039	4.8032	4.4127	4.2604	4.1865
	B2	IGA	12.2387	10.6259	9.6133	8.6079	7.6805	7.3821	7.267
		REF1	12.06	10.42	9.4561	8.5466	7.8331	7.561	7.4307
	B3	IGA	13.8287	12.1041	10.9865	9.8017	8.5867	8.2004	8.0641
		REF1	13.501	11.758	10.712	9.6759	8.7548	8.3957	8.2345
	B4	IGA	17.2298	15.4404	14.253	12.8027	11.0322	10.3673	10.1104
		REF1	17.718	15.423	14.04	12.67	11.473	11.011	10.802

REF1: (Hosseini-Hashemi *et al.* 2011)

in the frequency behavior at lower values, where the material properties vary significantly. As p increases, the material's composition approaches a more uniform distribution, resulting in minimal changes to the frequency, and thus, the impact of the h/a ratio becomes the dominant factor in determining the vibrational characteristics.

In Table 6, the natural frequency results are compared for four mode shapes for both iso-tropic and functionally graded material the boundary condition in this case is SSSS whereas for Table 7 and Table 8, the boundary condition is SSSC and SCSC. Table 9 compares first four natural frequency of SSSF. Table 10 and Table 11 presents the frequency of plate made up of combination of Al/ZrO_2 for SCSF and SFSF. The result shows the frequency is higher for SCSF compared to SFSF.

Fig. 2 illustrate the variation of the nondimensional fundamental natural frequency $\bar{\omega}$ of SSSS supported FG rectangular plates with side-to thickness ratios h/a for different power law index p. The frequency is maximum for the ceramic plate and minimum for the metallic plate. One of the main inferences from the analysis is that the response of FGM plates is intermediate to that of the ceramic and metal homogeneous plates.

Table 9 Comparison of first four natural frequency parameter for SSSF Al/ZrO_2 square plates

h/a	Mode	method	Power law index (P)						
			0	0.5	1	2	5	8	10
0.05	B1	IGA	3.5129	3.3111	3.2311	3.2265	3.2982	3.3003	3.2864
		REF1	3.5058	3.2995	3.2244	3.2208	3.2943	3.2983	3.2871
	B2	IGA	8.2662	7.7956	7.607	7.5913	7.7502	7.7537	7.7217
		REF1	8.2407	7.7596	7.5834	7.5721	7.7381	7.7457	7.7191
	B3	IGA	12.2926	11.5988	11.3186	11.2898	11.5145	11.5177	11.4704
		REF1	12.21	11.5	11.239	11.221	11.462	11.472	11.432
	B4	IGA	17.4227	16.446	16.0478	15.9982	16.2996	16.3025	16.2368
		REF1	17.328	16.329	15.96	15.927	16.255	16.265	16.208
0.1	B1	IGA	3.4467	3.252	3.1733	3.1649	3.2275	3.2285	3.2154
		REF1	3.4417	3.2424	3.1689	3.1631	3.2297	3.2321	3.2209
	B2	IGA	7.9368	7.5013	7.3189	7.2852	7.4013	7.4001	7.3715
		REF1	7.9147	7.4684	7.2999	7.2778	7.411	7.4114	7.3851
	B3	IGA	11.6397	11.0134	10.7452	10.6817	10.8233	10.8179	10.7775
		REF1	11.586	10.944	10.698	10.659	10.835	10.83	10.79
	B4	IGA	16.1981	15.349	14.9739	14.86	15.0079	14.9942	14.9409
		REF1	16.113	15.242	14.902	14.831	15.04	15.024	14.969
0.2	B1	IGA	3.2469	3.0738	2.9988	2.9793	3.0153	3.0133	3.0023
		REF1	3.2374	3.0598	2.9912	2.9789	3.0252	3.0231	3.0121
	B2	IGA	7.0473	6.6987	6.5337	6.4606	6.4816	6.4703	6.4495
		REF1	7.0065	6.648	6.5004	6.4542	6.512	6.4969	6.4722
	B3	IGA	9.9882	9.5202	9.2852	9.1528	9.1255	9.102	9.0755
		REF1	9.9002	9.4178	9.2125	9.1328	9.1763	9.1435	9.1068
	B4	IGA	13.3302	12.7379	12.4222	12.2103	12.1099	12.0703	12.038
		REF1	13.186	12.574	12.302	12.174	12.183	12.128	12.078

REF1: (Hosseini-Hashemi *et al.* 2011)

Table 10 Comparison of first four natural frequency parameter for SCSF Al/ZrO_2 square plates (b/h=1)

h/a	mode	method	Power law index (P)						
			0	0.5	1	2	5	8	10
0.05	B1	IGA	3.8111	3.5928	3.506	3.5003	3.5768	3.5788	3.5639
		REF1	3.7962	3.5732	3.492	3.4877	3.5665	3.5706	3.5584
	B2	IGA	9.8364	9.2819	9.0575	9.0332	9.2106	9.213	9.1754
		REF1	9.7487	9.1836	8.9755	8.9595	9.1491	9.1562	9.1244
	B3	IGA	12.4351	11.734	11.4505	11.4206	11.6461	11.6491	11.6013
		REF1	12.346	11.629	11.365	11.345	11.588	11.598	11.558
	B4	IGA	18.5329	17.5014	17.0777	17.0174	17.3221	17.3227	17.2494
		REF1	18.375	17.322	16.93	16.892	17.23	17.237	17.177

Table 11 Continued

h/a	mode	method	Power law index (P)						
			0	0.5	1	2	5	8	10
0.1	B1	IGA	3.7187	3.5103	3.4253	3.4144	3.4782	3.4788	3.4649
		REF1	3.7068	3.4936	3.4146	3.4074	3.4766	3.4786	3.4664
	B2	IGA	9.2735	8.7781	8.5644	8.5107	8.6166	8.6111	8.5791
		REF1	9.2021	8.6953	8.5006	8.467	8.6018	8.5964	8.5651
	B3	IGA	11.7504	11.1199	10.849	10.7831	10.9223	10.9162	10.8757
		REF1	11.691	11.045	10.797	10.756	10.931	10.926	10.886
	B4	IGA	17.0183	16.1414	15.7469	15.6116	15.7352	15.7162	15.6615
		REF1	16.886	15.987	15.632	15.549	15.746	15.723	15.664
0.2	B1	IGA	3.4549	3.2742	3.1943	3.1699	3.2007	3.1976	3.1862
		REF1	3.4383	3.2528	3.1804	3.1651	3.2092	3.2055	3.1936
	B2	IGA	7.8835	7.5175	7.3325	7.2262	7.2011	7.1812	7.1598
		REF1	7.7937	7.417	7.2553	7.1894	7.2183	7.1916	7.1628
	B3	IGA	10.0458	9.5773	9.341	9.2058	9.1744	9.1502	9.1236
		REF1	9.9541	9.4709	9.2647	9.1833	9.2242	9.1903	9.1533
	B4	IGA	13.7142	13.1208	12.7966	12.5639	12.4316	12.3857	12.353
		REF1	13.534	12.921	12.643	12.502	12.489	12.426	12.373

REF1: (Hosseini-Hashemi *et al.* 2011)

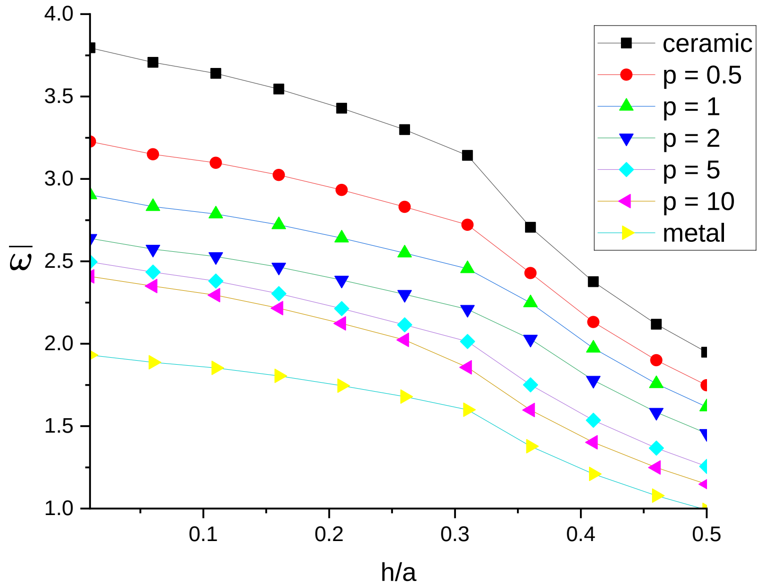

Fig. 2 Nondimensional fundamental natural frequency $\bar{\omega}$ of SSSS supported FG rectangular plates (b/a=2) (Al/Al_2O_3) as a function of side-tothickness ratio *a/h* for different power law index *p*

Fig. 3 presents the effect of power law index p on the tnondimensional fundamental natural frequency $\bar{\omega}$ and for different values of side-to thickness ratio h/a using the present theory. It is observed that an increase in the value of the power law index leads to a reduction of frequency.

Table 12 Comparison of first four natural frequency parameter for SFSF Al/ZrO_2 square plates (*b/h*=1)

h/a	mode	method	Power law index (P)						
			0	0.5	1	2	5	8	10
0.05	B1	IGA	2.903	2.736	2.6699	2.6665	2.7265	2.7283	2.7168
		REF1	2.8977	2.7268	2.6648	2.662	2.7233	2.7267	2.7174
	B2	IGA	4.8158	4.5408	4.4311	4.4228	4.5172	4.5195	4.5008
		REF1	4.7986	4.5176	4.415	4.409	4.5071	4.512	4.4965
	B3	IGA	10.8608	10.2468	9.9988	9.9735	10.1733	10.1769	10.1352
		REF1	10.809	10.182	9.9505	9.933	10.145	10.154	10.119
	B4	IGA	11.6433	10.9856	10.7204	10.6935	10.9079	10.9113	10.8663
		REF1	11.561	10.888	10.641	10.624	10.853	10.863	10.826
0.1	B1	IGA	2.8603	2.6978	2.6325	2.6266	2.6806	2.6818	2.6708
		REF1	2.8569	2.6906	2.6296	2.6253	2.682	2.6844	2.675
	B2	IGA	4.6679	4.4082	4.3013	4.2857	4.362	4.3623	4.345
		REF1	4.657	4.3908	4.2915	4.2811	4.3656	4.3674	4.3521
	B3	IGA	10.2837	9.7281	9.4911	9.4383	9.5714	9.5674	9.5312
		REF1	10.246	9.6764	9.4582	9.4233	9.583	9.5806	9.5464
	B4	IGA	11.0531	10.4559	10.2013	10.1423	10.2832	10.2784	10.2402
		REF1	11.002	10.39	10.157	10.121	10.292	10.288	10.251
0.2	B1	IGA	2.7255	2.578	2.5152	2.5012	2.5361	2.535	2.5255
		REF1	2.7184	2.5672	2.5096	2.5006	2.5429	2.5419	2.5327
	B2	IGA	4.2788	4.058	3.9589	3.9254	3.9581	3.9536	3.9398
		REF1	4.265	4.0376	3.9474	3.926	3.9764	3.971	3.9563
	B3	IGA	8.8709	8.4458	8.236	8.1335	8.1387	8.1213	8.0962
		REF1	8.8171	8.3769	8.1902	8.1217	8.177	8.1549	8.1241
	B4	IGA	9.5458	9.098	8.8737	8.7509	8.7295	8.6716	8.6522
		REF1	9.4629	8.9983	8.802	8.7282	8.7752	8.7451	8.7101

REF1: (Hosseini-Hashemi *et al.* 2011)

The highest frequency values are obtained for full ceramic beams ($p = 0$) while the lowest frequency values are obtained for full metal beams ($p \to \infty$). This is due to the fact that an increase in the value of the power law index results in a decrease in the value of elasticity modulus. In other words, the plate becomes flexible as the power law index increases, thus decreasing the frequency values. It can be also seen that the side-to thickness ratio *h/a* has a considerable effect on the non-dimensional fundamental natural frequency $\overline{\omega}$ where this latter is reduced with decreasing *h/a*. This dependence is related to the effect of shear deformation.

5. Conclusions

The study introduces an efficient computational method utilizing iso-geometric analysis (IGA) with NURBS basis functions for analyzing the free vibration of functionally graded plates. Extensive numerical examples and comparisons with existing models demonstrate the method's effectiveness in accurately predicting the natural frequencies of such plates. Moreover, the study

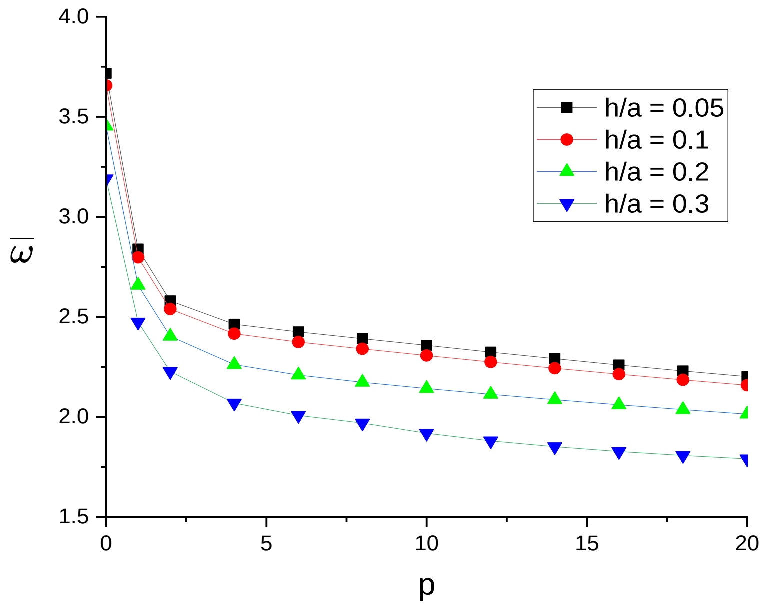

Fig. 3 Nondimensional fundamental natural frequency $\overline{\omega}$ of SSSS supported FG rectangular plates (b=2a) (Al/Al_2O_3) as a function of power law index p for different *h/a*

explores the impact of different parameters on the frequency behavior. Increasing the exponent (*p*) in the composition of ceramic and metal materials results in a decrease in the proportion of ceramics and an increase in the proportion of metals. Additionally, the study finds that the effect of the ratio of plate thickness to plate length (*h/a*) on frequency is more significant compared to the grading parameter *p*. Lower *p* values correspond to larger decrements in frequency, while higher *p* values show less variation in the results.

Furthermore, comparing the two material combinations, Al/Al_2O_3 and Al/ZrO_2, the natural frequency is higher when $Al2O_3$ is used as the reinforcement. The natural frequency is highest under the SCSC boundary condition, followed by SSSC and SSSS. Overall, these findings provide valuable insights into the frequency behavior of functionally graded plates and can inform the selection and design of materials for specific applications.

References

Ait Atmane, H., Tounsi, A., Mechab, I. and Adda Bedia, E.A. (2010), "Free vibration analysis of functionally graded plates resting on Winkler-Pasternak elastic foundations using a new shear deformation theory", *Int. J. Mech. Mater. Des.*, **6**(2), 113-121. https://doi.org/10.1007/s10999-010-9110-x.

Alghanmi, R. (2023), "Hygrothermal bending analysis of sandwich nanoplates with FG porous core and piezomagnetic faces *via* nonlocal strain gradient theory", *Nanotechnol. Rev.*, **12**(1), 20230123. https://doi.org/10.1515/ntrev-2023-0123.

Alghanmi, R.A. (2022), "Nonlocal strain gradient theory for the bending of functionally graded porous nanoplates", *Mater.*, **15**(23), 8601. https://doi.org/10.3390/ma15238601.

Alghanmi, R.A. and Aljaghthami, R.H. (2024), "A four-variable shear deformation theory for the static analysis of FG sandwich plates with different porosity models", *Math. Comput. Appl.*, **29**(2), 20.

https://doi.org/10.3390/mca29020020.

Balobanov, V., Khakalo, S. and Niiranen, J. (2016), "Isogeometric analysis of gradient-elastic 1D and 2D problems", *General. Continua Model. Class. Adv. Mater.*, 37-45. https://doi.org/10.1007/978-3-319-31721-2_3.

Bazilevs, Y., Calo, V.M., Zhang, Y. and Hughes, T.J.R. (2006), "Isogeometric fluid-structure interaction analysis with applications to arterial blood flow", *Comput. Mech.*, **38**(4-5), 310-322. https://doi.org/10.1007/s00466-006-0084-3.

Benachour, A., Daouadji, H., Atmane, H. A., Tounsi, A. and Sid Ahmed, M. (2011), "A four-variable refined plate theory for free vibrations of functionally graded plates with arbitrary gradient", *Compos. Part B: Eng.*, **42**(6), 1386-1394. https://doi.org/10.1016/j.compositesb.2011.05.032.

Bennai, R., Ait Atmane, H., Ayache, B., Tounsi, A., Adda Bedia, E.A. and Al-Osta, M.A. (2016), "Free vibration response of functionally graded Porous plates using a higher-order Shear and normal deformation theory", *Earthq. Struct.*, **16**(5), 547-561. https://doi.org/10.12989/eas.2019.16.5.547.

Bennai, R., Fourn, H., Nebab, M., Ait Atmane, R., Mellal, F., Ait Atmane, H., Benadouda, M. and Tounsi, A. (2022), "On the wave dispersion and vibration characteristics of FG plates resting on elastic Kerr foundations via HSDT", *Adv. Concrete Constr.*, **14**(3), 169-183. https://doi.org/10.12989/acc.2022.14.3.169.

Buffa, A. and Sangalli, G. (2016), *IsoGeometric Analysis: A New Paradigm in the Numerical Approximation of PDEs: Cetraro*, Springer, Italy.

Cazenave, M. (2013), *Méthode des Eléments Finis-2e éd.: Approche Pratique en Mécanique des Structures*, Dunod.

Chen, L., Dornisch, W. and Klinkel, S. (2014), "A NURBS based collocation approach for SB-FEM", *Int. Center Numer. Meth. Eng.*, **2**, 2469-2480.

De Boor, C. (1972), "On calculating with B-splines", *J. Approx. Theory*, **6**(1), 50-62.

Djilali Djebbour, K., Ait Atmane, H., Nebab, M., Bennai, R., Hadji, L. and Dahmane, M. (2024), "Effect of porosity distribution on free vibration of functionally graded plates: an accurate application of HSDT theory", *Stud. Eng. Exact Sci.*, **5**(2), e6915. https://doi.org/10.54021/seesv5n2-114.

Draouche, K, Ait Amar Meziane, M., Hadji, L., Ait Atmane, H., Bennai, R. and Madan, R. (2024), "Effect of porosity and boundary conditions on dynamic characteristics of cracked plates made of functionally graded materials", *Adv. Concrete Constr.*, **18**(3), 175-190. https://doi.org/10.12989/acc.2024.18.3.175.

Cottrell, J.A., Reali, A., Bazilevs, Y. and Hughes, T.J.R. (2006), "Isogeometric analysis of structural vibrations", *Comput. Meth. Appl. Mech. Eng.*, **195**(41-43), 5257-5296. https://doi.org/10.1016/j.cma.2005.09.027.

Hosseini-Hashemi, Sh., Fadaee, M. and Atashipour, S.R. (2011), "A new exact analytical approach for free vibration of Reissner-Mindlin functionally graded rectangular plates", *Int. J. Mech. Sci.*, **53**(1), 11-22. https://doi.org/10.1016/j.ijmecsci.2010.10.002.

Hosseini-Hashemi, Sh., Rokni Damavandi Taher, H., Akhavan, H. and Omidi, M. (2010), "Free vibration of functionally graded rectangular plates using first-order shear deformation plate theory", *Appl. Math. Model.*, **34**(5), 1276-1291. https://doi.org/10.1016/j.apm.2009.08.008.

Hussain, M. and Selmi, A. (2020), "Effect of Pasternak foundation: Structural modal identification for vibration of FG shell", *Adv. Concrete Constr.*, **9**(6), 569-576. https://doi.org/10.12989/acc.2020.9.6.569.

Hughes, T.J.R., Cottrell, J.A. and Bazilevs, Y. (2005), "Isogeometric analysis: CAD, finite elements, NURBS, exact geometry and mesh refinement", *Comput. Meth. Appl. Mech. Eng.*, **194**(39-41), 4135-4195. https://doi.org/10.1016/j.cma.2004.10.008.

Hughes, T.J.R., Reali, A. and Sangalli, G. (2010), "Efficient quadrature for NURBS-based isogeometric analysis", *Comput. Meth. Appl. Mech. Eng.*, **199**(5-8), 301-313. https://doi.org/10.1016/j.cma.2008.12.004.

Kacprzyk, Z. and Ostapska-Łuczkowska, K. (2014), "Isogeometric analysis as a new FEM formulation-simple problems of steady state thermal analysis", *Procedia Eng.*, **91**, 87-92. https://doi.org/10.1016/j.proeng.2014.12.018.

Khadimallah, M.A., Hussain, M., Al-Thobiani, F., Elbahar, M., Al Naim, A.F., Elimame, E., Harbaoui, I.

and Tounsi, A. (2021), “An innovative system for novel vibration of rotating FG shell with combination of fraction laws”, *Adv. Concrete Constr.*, **12**(2), 157-165. https://doi.org/10.12989/acc.2021.12.2.157.

Kiani, M. and Arefi, M. (2023), “Nonlocal bending characteristics of nanoplate reinforced by functionally graded GPLs exposed to thermo-mechanical loads resting on the Pasternak’s foundation”, *Adv. Concrete Constr.*, **15**(2), 97-114. https://doi.org/10.12989/acc.2023.15.2.097.

Kazemi, H.S. and Tavakkoli, S.M. (2023), “A new algorithm for design of support structures in additive manufacturing by using topology optimization”, *Struct. Eng. Mech.*, **86**(1), 93-107. https://doi.org/10.12989/sem.2023.86.1.093.

Khalafi, V. and Fazilati, J. (2021), “Free vibration analysis of functionally graded plates containing embedded curved cracks”, *Struct. Eng. Mech.*, **79**(2), 157-168. https://doi.org/10.12989/sem.2021.79.2.157.

Kiran, M.C. and Kattimani, S. (2017), “Buckling characteristics of multilayered magneto-electro-elastic plate”, *Struct. Eng. Mech.*, **64**(6), 697-714. https://doi.org/10.12989/sem.2017.64.6.697.

Kiran, M.C. and Kattimani, S. (2018a), “Buckling analysis of skew magneto-electro-elastic plates under in-plane loading”, *J. Intel. Mater. Syst. Struct.*, **21**, 1-17. https://doi.org/10.1177/1045389X18758191.

Kiran, M.C., Kattimani, S. and Vinyas, M. (2018b), “Porosity influence on structural behavior of skew functionally graded magneto-electro-elastic plate”, *Compos. Struct.*, **191**, 36-77. https://doi.org/10.1016/j.compstruct.2018.02.023.

Kiran, M.C. and Kattimani, S. (2018c), “Free vibration and static analysis of functionally graded skew magneto-electro-elastic plate”, *Smart Struct. Syst.*, **21**(4), 493-519. https://doi.org/10.12989/sss.2018.21.4.493.

Kiran, M.C. and Kattimani, S. (2018d), “Assessment of porosity influence on vibration and static behavior of functionally graded magneto-electro-elastic plate: A finite element study”, *Eur. J. Mech. Solid.*, **71**, 258-277. https://doi.org/10.1016/j.euromechsol.2018.04.006.

Kiran, M.C. and Kattimani, S. (2018e), “Assessment of vibrational frequencies and static characteristics of multilayered skew magneto-electro-elastic plates: A finite element study”, *Iran J. Sci. Technol.: Trans. Mech. Eng.*, **44**(1), 61-82. https://doi.org/10.1007/s40997-018-0250-1.

Kiran, M.C. and Kattimani, S. (2018f), “Free vibration of multilayered magneto-electro-elastic plates with skewed edges using layerwise shear deformation theory”, *Mater. Today Proc.*, **191**, 21248-21255. https://doi.org/10.1016/j.matpr.2018.06.525.

Kolman, R., Sorokin, S., Bastl, B., Kopačka, J. and Plešek, J. (2015), “Isogeometric analysis of free vibration of simple shaped elastic samples”, *J. Acoust. Soc. Am.*, **137**(4), 2089-2100. https://doi.org/10.1121/1.4916199.

Lahdiri, A. and Kadri, M. (2022), “Free vibration behaviour of multi-directional functionally graded imperfect plates using 3D isogeometric approach”, *Earthq. Struct.*, **22**(5), 538. https://doi.org/10.12989/eas.2022.22.5.538.

Lakel, A., Hadji, L., Avcar, M., Ait Atmane, H. and Madan, R. (2024), “The Natural Frequency Analysis of FG-GNPR nanoplates under different boundary conditions”, *Adv. Nano Res.*, **17**(6) 533-546. https://doi.org/10.12989/anr.2024.17.6.533.

Liu, H., Zhu, X. and Yang, D. (2016), “Isogeometric method based in-plane and out-of-plane free vibration analysis for Timoshenko curved beams”, *Struct. Eng. Mech.*, **59**(3), 503-526. https://doi.org/10.12989/SEM.2016.59.3.503.

Les, P. and Wayne, T. (1997), *The NURBS Book*, Springer-Verlag, Berlin.

Matsunaga, H. (2008), “Free vibration and stability of functionally graded plates according to a 2-D higher-order deformation theory”, *Compos. Struct.*, **82**(4), 499-512. https://doi.org/10.1016/j.compstruct.2007.01.030.

Meski, K., Zouatnia, N., Menasria, A., Mamen, B., Hadji, L., Bouhadra, A. and Ait Atmane, H. (2024), “Static behavior of functionally graded sandwich beam with 1D-FG skins and ceramic core using a new quasi-3D HSDT”, *Adv. Concrete Constr.*, **18(**6), 399-410. https://doi.org/10.12989/acc.2024.18.6.399.

Ould Larbi, L., Saad, M., Zouatnia, N., Hadji, L. and Sayyad, A.S. (2024), “A simple refined plate theory for buckling problems of in-plane bi-directional functionally graded plates with porosity under various boundary conditions", *Mech. Adv. Mater. Struct.*, 1-10. https://doi.org/10.1080/15376494.2024.2346946.

Pradyumna, S. and Bandyopadhyay, J. (2008), "Free vibration analysis of functionally graded curved panels using a higher-order finite element formulation", *J. Sound Vib*, **318**(1-2), 176-192. https://doi.org/10.1016/j.jsv.2008.03.056.

Rauen, M., Machado, R.D. and Arndt, M. (2013), "Isogeometric analysis of free vibration of bars", *22nd International Congress of Mechanical Engineering*, November.

Selmi, A. (2021), "Free vibration of bi-dimensional functionally graded simply supported beams", *Adv. Concrete Constr.*, **12**(3), 195-205. https://doi.org/10.12989/acc.2021.12.3.195.

Shojaee, S., Ghelichi, M. and Izadpanah, E. (2013), "Combination of isogeometric analysis and extended finite element in linear crack analysis", *Struct. Eng. Mech.*, **48**(1), 125-150. https://doi.org/10.12989/sem.2013.48.1.125.

Shojaee, S., Izadpanah, E., Valizadeh, N. and Kiendl, J. (2012), "Free vibration analysis of thin plates by using a NURBS-based isogeometric approach", *Finite Elem. Anal. Des.*, **61**, 23-34. https://doi.org/10.1016/j.finel.2012.06.005.

Shojaee, S. and Valizadeh, N. (2012), "NURBS-based isogeometric analysis for thin plate problems", *Struct. Eng. Mech.*, **41**(5), 617-632. https://doi.org/10.12989/sem.2012.41.5.617.

Son, T. and Huu-Tai, T. (2019), "Free-vibration analysis of multi-directional functionally graded plates based on 3D isogeometric analysis", *J. Sci. Technol. Civil Eng. (STCE)-NUCE*, **13**(2), 1-11. https://doi.org/10.31814/stce.nuce2019-13(2)-01.

Vel, S.S. and Batra, R. (2004), "Three-dimensional exact solution for the vibration of functionally graded rectangular plates", *J. Sound Vib.*, **272**(3-5), 703-730. https://doi.org/10.1016/S0022-460X(03)00412-7.

Zhao, X., Lee, Y. and Liew, K.M. (2009), "Free vibration analysis of functionally graded plates using the element-free kp-Ritz method", *J. Sound Vib.*, **319**(3-5), 918-939. https://doi.org/10.1016/j.jsv.2008.06.025.

Zouatnia, N., Hadji, L., Atmane, H.A. and Larbi, L.O. (2024), "Impact of porosity distribution and grading parameters on free vibration of functionally graded beams", *Stud. Eng. Exact Sci.*, **5**(2), e6945. https://doi.org/10.54021/seesv5n2-122.